Apophyllite group: effects of chemical substitutions on dehydration behaviour, recrystallization products and cell parameters

GISELLE F. MARRINER

Department of Geology, Royal Holloway and Bedford New College, Egham Hill, Egham, Surrey TW20 0EX

JOHN TARNEY

Department of Geology, University of Leicester, Leicester LE1 7RH

AND

J. IAN LANGFORD

School of Physics and Space Research, University of Birmingham, Birmingham B15 2TT

Abstract

The effects of (OH)/F substitutions on thermally induced reactions in the apophyllite group have been investigated using TGA and DTA methods, supplemented by X-ray diffraction, infra-red and other techniques to identify the products of reaction. The samples studied cover the range between fluorapophyllite and hydroxyapophyllite, and include some unusual ammonium varieties. The presence or absence of fluorine exerts a major control on thermally induced reactions, not only during low-temperature dehydration, but also on high temperature recrystallization reactions up to 900°C+. All apophyllites dehydrate in two stages, the first being loss of a proportion of the water with only minor distortion of the crystal lattice, whereas the second results in total collapse into an amorphous material. Higher fluorine concentrations stabilize the structure, shifting dehydration reactions to higher temperatures, and permitting more water molecules to be lost during the first stage without destruction of the structure. Fluorine is not lost during the second-stage dehydration, as previously believed, but most is retained and influences subsequent recrystallization reactions.

Dehydrated hydroxyapophyllites remain amorphous until *ca.* 900°C, when high-temperature wollastonite crystallizes. Fluorapophyllites initially form a metastable $CaF_2.SiO_2$ phase by 700°C, low-temperature wollastonite by 800°C, both disappearing above 900°C when fluorine loss occurs and high-temperature wollastonite is produced. TGA and DTA provide simple methods of distinguishing between hydroxy- and fluorapophyllites.

Ammonian apophyllites, with up to 25% of the stoichiometric K^+ replaced by NH_4^+ (in the samples studied), can be recognized by their DTA patterns, the endothermic peak for the second stage reaction being significantly reduced, and that for the first, dehydration, stage being correspondingly enhanced. Such samples have weight losses well above the calculated water content, the excess being due to evolution of ammonia. Ammonian varieties also have an extra infra-red absorption band at 1460 cm^{-1}.

KEYWORDS: apophyllite, fluorapophyllite, hydroxyapophyllite, ammonian apophyllite, dehydration, thermal reactions, wollastonite.

Mineralogical Magazine, December 1990, Vol. 54, pp. 567–577

Introduction

APOPHYLLITE [$KCa_4Si_8O_{20}F.8H_2O$], a hydrous sheet-structured mineral, is frequently found associated with zeolites in rocks affected by low temperature hydrothermal activity. Like many zeolites, it releases an appreciable proportion of its loosely bonded water at relatively low temperatures without significant breakdown of the crystal lattice. The remainder is not released until much higher temperatures. The initial crystal structure determination by Taylor and Náray-Szabò (1931) suggested no apparent difference in the location of the eight water molecules in the structure which might account for this behaviour.

It is now known that there is some variation in the composition of apophyllite, particularly with regard to fluorine content. Dunn *et al.* (1978) have redefined the apophyllite group in terms of a solid solution series between the two end-members: fluorapophyllite, $KCa_4Si_8O_{20}F.8H_2O$, and hydroxyapophyllite, $KCa_4Si_8O_{20}(OH).8H_2O$. Refinement of the structure of hydroxyapophyllite by Rouse *et al.* (1978) showed that it does not differ significantly from fluorapophyllite. They concluded that the two end-members can be distinguished only by chemical means.

To try to resolve the uncertainty concerning the location of the water molecules, we have investigated the thermal behaviour of some 35 different apophyllites spanning the range between fluor- and hydroxyapophyllite. The results show that the degree of OH–F substitution influences not only the temperatures of the two stages of dehydration, but also the proportion of water lost during each stage and even the initial recrystallization products. Thermal analysis indeed provides a relatively simple way of distinguishing between different members of the apophyllite series. Moreover the results indicate that there is another, previously unsuspected, type of substitution in the apophyllite group, where NH_4+ replaces K+.

Previous work

Crystal structure. The apophyllite structure determined by Taylor and Náray-Szabò (1931) was further refined by Colville *et al.* (1971), Chao (1971), Prince (1971) and Bartl and Pfeifer (1976), and by Rouse *et al.* (1978) for hydroxyapophyllite. The mineral is normally tetragonal, space group *P4/mnc*, with cell parameters listed in Table 1; however, where significant amounts of Na substitute for K, the lattice is distorted and the symmetry reduced to orthorhombic (Matsueda *et al.*, 1981). The structure consists of continuous sheets of SiO_4 tetrahedra lying parallel to (001), but in contrast to the 6-membered rings of the mica group, these sheets are made up of 4- and 8-membered rings of silica tetrahedra, with alternate 4-membered rings pointing up and down the *c*-axis (Fig. 1). The sheets are linked together by Ca ions bonded to two oxygens from each of the two adjacent sheets, one (OH,F) and two H_2O molecules. Each (F,OH) ion is coordinated to four coplanar Ca ions, whereas each K ion is surrounded by eight H_2O molecules.

Thermal behaviour. Taylor and Náray-Szabò (1931) observed that half the water content is lost at 240–250°C, but that the partly dehydrated crystals recover water slowly, if incompletely. Aumento (1965) ascertained that the two main dehydration stages occur at temperatures of 250 and 350°C respectively, and that above 250°C the intensities of the X-ray reflections decreased progressively with increasing temperature until the material became amorphous above 370°C. A multi-stage dehydration process is typical of minerals where the water molecules are held in more than one structural site (Sarig, 1973), so that the loss of water in two stages in apophyllite is therefore suggestive of two distinct sites (Chao, 1971). However, refinement of the crystal structure using X-ray diffraction in conjunction with infra-red studies of O–H bonding (Colville *et al.*, 1971) and determination of hydrogen ion positions by neutron diffraction (Prince, 1971) indicate unequivocally that only one such site exists. Chao (1971) concluded that, after losing half the water molecules, the mineral changes to another compound, structurally identical to apophyllite except in the environment of the water molecules. A further uncertainty concerns the extent to which fluorine is lost during the second-stage reaction. On the basis of his neutron diffraction studies, Prince (1971) concluded that hydrogen ions were associated with a proportion of the fluorine ions, and he used this to account for the presence of hydrogen fluoride in the evolved gases during the second-stage dehydration. However, Bartl and Pfeiffer (1976) suggested that Prince's sample was not the pure fluorapophyllite end-member, and hence that a proportion of the fluorine sites were occupied by hydroxyl ions.

Kinetic studies of the dehydration behaviour, reported by Lacy (1965), showed that apophyllite loses not half, but 5/8ths of its structural water during the first stage of dehydration. The activation energy of this first stage reaction was found to be 14 kcal/mole, only slightly higher than that usually found for the loss of "zeolitic" water, whereas that for the second stage was 63 kcal/mole. The activation energy of the second-stage reaction is too high to be due simply to the loss

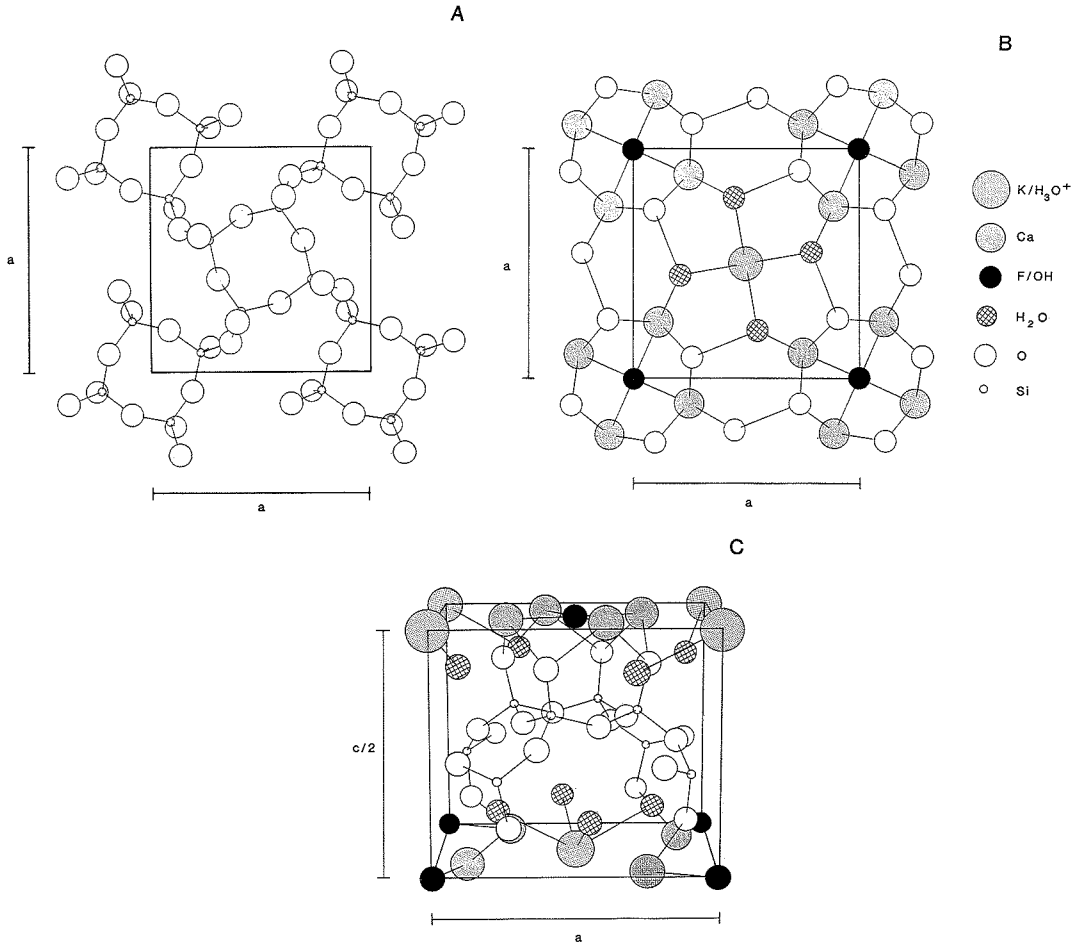

FIG. 1. Structure of apophyllite [$KCa_4(Si_4O_{10})_2(F/OH).8H_2O$] based on Taylor and Náray-Szabò (1931): A, (001) silicon–oxygen layer showing 4-member Si–O rings surrounded by 8-member Si–O rings; B, (001) cation layer; C, general layered structure viewed along (100). [Erratum in proof: *for* K/H_3O^+ *read* K/NH_3]

Table 1. Cell dimensions for the apophyllite group

	a	b	c	F(%)
Fluorapophyllite[a]	8.963(2)	-	15.804(2)	2.20
Hydroxyapophyllite[b]	8.978(3)	-	15.830(1)	0.0
Natroapophyllite[c]	8.875(4)	8.881(6)	15.79(1)	2.27
Fluorapophyllite GM01	8.969(1)	-	15.796(2)	2.08
Apophyllite GM05	8.976(4)	-	15.825(6)	1.28
Hydroxyapophyllite GM24	8.985(2)	-	15.875(3)	0.56
NH_4- hydroxyapophyllite GM25	8.988(2)	-	15.888(3)	0.07
NH_4- fluorapophyllite GM13	8.978(2)	-	15.781(3)	1.94

[a]From Colville *et al.* (1971), [b]from Dunn *et al.* (1978), [c]from Matsueda *et al.* (1981)

Table 2. Chemical analyses of apophyllites

Sample	SiO_2	Al_2O_3	CaO	Na_2O	K_2O	$(NH_4)_2O$	F	H_2O	O for F	Total	[BM Ref]
Fluoroapophyllite - Hydroxyapophyllite series											
AP-F	**52.99**	**0.00**	**24.74**	**0.00**	**5.19**	**-**	**2.09**	**15.87**	**-0.88**	**100.00**	**(ideal)**
GM26*	52.72	0.28	24.59	0.21	4.96	-	2.12	16.00	-0.89	99.39	BM93563
GM1*	52.88	0.28	24.89	0.26	4.77	-	2.08	16.40	-0.88	100.58	BM43729
GM19	53.79	0.56	24.76	0.36	4.24	-	2.07	16.28	-0.86	100.20	BM1914191
GM29	52.19	0.00	24.73	0.02	4.82	-	2.05	16.41	-0.87	99.35	BM55265
GM20	51.63	0.11	24.52	0.15	4.83	-	2.05	16.49	-0.87	98.91	BM1914967
GM14	52.73	0.13	24.95	0.29	4.20	-	2.05	16.27	-0.87	99.75	BM47936
GM15	52.20	0.43	24.95	0.17	4.69	-	2.05	17.00	-0.87	100.62	BM33777
GM18	52.97	0.18	24.82	0.07	4.91	-	2.04	16.28	-0.86	100.41	BM19271079
GM23	52.32	0.23	24.43	0.16	4.91	-	2.00	15.70	-0.84	98.91	BM1963237
GM2	52.72	0.09	24.79	0.04	4.94	-	1.99	15.90	-0.84	99.63	BM1972354
GM31*	52.83	0.27	24.74	0.15	5.18	-	1.99	16.22	-0.83	100.55	[KCLond]
AP1*	53.00	0.40	24.93	0.18	4.91	-	1.99	16.22	-0.83	100.80	[BUniv]
GM4	52.65	0.26	24.58	0.12	4.77	-	1.95	15.80	-0.82	99.31	BM1914476
GM7	50.67	0.11	24.71	0.04	4.97	-	1.90	15.80	-0.81	97.39	BM40345
AP2	53.08	0.00	24.97	0.01	3.66	-	1.85	15.40	-0.83	98.14	[BUniv]
GM16	51.69	0.09	24.44	0.12	4.82	-	1.83	15.60	-0.77	99.82	BM66244
AP9*	53.96	0.29	23.11	0.26	4.18	-	1.80	16.20	-0.76	99.04	[BCLond]
AP6	50.06	0.95	24.38	0.13	4.36	-	1.79	16.20	-0.76	97.11	BM47692
AP8*	53.09	0.25	24.38	0.09	4.92	-	1.70	16.30	-0.71	100.02	BM28156
AP5	52.61	0.03	24.63	0.03	4.72	-	1.43	17.60	-0.42	100.63	[BUniv]
GM27	52.87	0.26	24.91	0.10	4.98	-	1.38	17.05	-0.58	100.88	BM93525
GM6*	53.17	0.31	25.02	0.03	5.05	-	0.95	15.60	-0.40	99.73	BM1965364
GM24	52.31	0.84	24.81	0.36	4.74	-	0.56	16.60	-0.24	100.98	BM1950477
GM30	50.94	0.10	24.54	0.07	4.97	-	0.56	17.00	-0.24	97.94	BM41713
AP7	52.13	0.01	25.01	0.01	4.98	-	0.12	16.90	-0.04	99.12	BM62762
GM21	52.46	0.08	24.72	0.05	4.98	-	0.05	17.60	-0.02	99.88	BM62761
AP4	52.68	0.02	24.94	0.04	4.90	-	0.03	16.80	-0.01	99.40	[BUniv]
AP-OH	**53.11**	**0.00**	**24.79**	**0.00**	**5.20**	**-**	**0.00**	**16.90**	**0.00**	**100.00**	**(ideal)**
Ammonian apophyllites											
GM10	52.36	0.55	24.61	0.30	4.45	0.05	2.05	16.55	-0.87	100.05	BM1952111
GM3	52.10	0.50	24.77	0.23	4.47	0.10	2.01	17.34	-0.85	100.67	BM1914775
GM5*	53.17	0.19	24.65	0.08	4.85	0.11	1.28	16.43	-0.54	100.22	BM1914912
GM17	52.98	0.38	24.61	0.25	4.42	0.13	2.02	17.11	-0.85	101.05	BM191696
GM25*	53.00	0.21	24.86	0.12	4.28	0.41	0.07	17.43	-0.03	100.43	BM19271008
GM12	52.74	0.01	24.84	0.02	3.67	0.67	1.67	16.76	-0.70	99.79	BM19141461
GM13	53.07	0.26	25.33	0.12	3.38	0.68	1.94	17.66	-0.82	101.60	BM39815
GM11	52.47	0.28	24.79	0.15	3.62	0.72	1.80	16.93	-0.76	100.00	BM19141454

*Major element analysis by ICP (otherwise by electron microprobe), F & NH_3 by colorimetry & water by TGA.

Location of samples: GM1 Blomindon, King's Co. Nova Scotia; GM2 Gaspe Cu Mine, Quebec; GM3 Snake Hill, N Bergen, Hudson Co., New Jersey; GM4 Phoenix Mine, Keweenaw Co, Michigan; GM5 Great Notch 3, Passsaic Co, New Jersey; GM6 Fairfax Quarry, Centreville, Fairfax Co, Viginia; GM7 Bergen Hill, Hudson Co., New Jersey; GM10 Laguna, Santa Catrina, Brazil; GM11 Guanejuato City, Mexico; GM12 Refugio Mine, Lahuz, Guanejuato State, Mexico; GM13 Mexico; GM14, GM16 & AP6 Syhadree Mts, Bombay, India; GM15 Railway cuttings, Syhadree Mts, Bombay; GM17 Samson Mine, Andreasburg, Harz, Germany; GM18 Niederrothweil, Kaiserstuhl, Baden, Germany; GM19 Andreasburg, Harz, Germany; GM20 Frumm Bach, Selser Alpe, Rozen, Tyrol; GM21 & AP7 De Beers Diamond Mine, Kimberley, S. Africa; GM23 Korsnas Lead Mine, Svartoren, Vaasa Prov., Finland; GM24 Gikenmine, Sulitjela, Nordland, Norway; GM25 Karatut, Disko Is., Godhavn Distr., W. Greenland; GM26 Hesto, Faeroe Islands; GM27 Eide, Ostera, Faeroe Islands; GM29 Marienberg, Aussig, Bohemia; GM30 Storr Mount, *Isle of Skye; GM31 Meldon Quarry Okehampton*; AP1 (unknown); AP2 (Goodchild Coll., unknown); AP4 S. Africa; AP5 (unknown); AP8 Bergen Hill, Hudson Co, New Jersey; AP9 (unknown)

of molecular water and was explained in terms of rupture of Si–O–Si bonds during breakdown of the lattice. Lacy demonstrated diagrammatically how 5 of the 8 water molecules could be removed without fundamental destruction of the crystal lattice of apophyllite. The sample studied (AP1, Table 2) has been found during this work to be a fairly pure fluorapophyllite.

Apophyllite compositions

A total of 35 different apophyllite samples were analysed in order to relate composition to dehydration behaviour. Major and minor elements were determined by standard electron microprobe and ICP techniques, as described by Reed (1976) and by Walsh (1979) and Walsh and Howie (1980) respectively. The instruments used were a Jeol JXA-8600S wavelength spectrometer and a Philips PV8210 plasma emission spectrometer. Fluorine was analysed by both electron microprobe and standard colorimetric techniques, the latter involving the use of alizarin fluorine blue lanthanum complex or xylenol orange, following fusion with sodium carbonate. Measurements were made using a Philips SP500 spectrophotometer. Ammonia was analysed by an indo-phenol colorimetric technique after Mann (1963), and by IR. Water contents were measured as weight loss minus NH_3 on a Stanton-Redcroft thermobalance.

Apophyllites present their own special difficulties as regards chemical analysis. Their high fluorine contents lead to erroneous SiO_2 results by ICP because SiF_4 tends to be lost during sample preparation. The high volatile contents, and low temperatures of dehydration, cause problems during microprobe analysis because samples decompose under the electron beam, thus necessitating use of a defocussed 15 μm beam and current reduced

to 30 nA. There is a slight bias to low SiO_2 using ICP techniques and to lower fluorine using microprobe techniques; agreement for other elements was good.

The samples cover the entire compositional range from pure fluorapophyllite (2.12% F) to almost pure hydroxyapophyllite (0.025% F), and analyses are given in Table 2. Notably in such a random selection of samples of this mineral from world-wide locations, fluorapophyllites are dominant, and the samples cluster near the fluorapophyllite end-member. Most samples conform well to the ideal formula for the apophyllite group, with only limited substitution of Al for Si, or Na for K. Similar substitutions were noted by Dunn *et al.* (1978). but Matsueda *et al.* (1981) and Miura *et al.* (1981) described a Na analogue, natroapophyllite, and a continuous pseudo-solid solution series between this and K-rich fluorapophyllite.

Several samples (Table 2), predominantly from Mexico, are deficient in K_2O by more than 25% of that required by the ideal formula. None of the elements commonly substituting for K (such as Na, Rb, Sr or Ba) was found to be present in more than trace amounts. However, all these samples record excess weight losses on heating: mostly between 17.2 and 18.1% total loss compared with the theoretical H_2O contents of 15.9 and 16.9% for the fluor- and hydroxyapophyllite end-members respectively. This correlation of excess weight-loss with low K_2O suggests the missing component is volatile. Infra-red spectra of the K-deficient apophyllites exhibit an extra absorption band in the region 1466–1459 cm^{-1}, attributable to the NH_4 deformation band. The intensity of this band is directly proportional to the deficiency in K_2O. Chemical analysis (Table 2) demonstrates that up to 25% of the potassium is replaced by ammonia. This substitution is well known in other silicates, particularly the micas (Yamamento and Nakahira, 1966; Duit *et al.*, 1986; D. Morgan, *pers. comm.*) and the feldspars (Soloman and Rossman, 1988). Whether a complete substitution series exists with the ammonium ion totally replacing potassium is not known. The most extreme substitution observed (GM13 in Table 2) amongst the 35 samples studied has one quarter of the ideal formula K^+ by NH_4^+. Such variants will be referred to as 'ammonian apophyllites".

Cell parameters in relation to composition. Dunn *et al.* (1978) found a small increase in the *a* and *c* cell dimensions for hydroxyapophyllite compared with those determined by Colville *et al.* (1971) for fluorapophyllite. Dunn *et al.* performed a least-squares refinement from powder diffraction data using quartz as an internal standard. For the present work, X-ray diffraction data were obtained for five powder samples, selected to represent a wide range of composition. A Picker 2-circle high-resolution powder diffractometer with Cu-$K\alpha_1$ radiation and an incident-beam focussing monochromator was used; systematic errors were removed by means of an Ag internal standard. The data were refined by using the suite of programs of Langford (1971) and the cell parameters are given in Table 1.

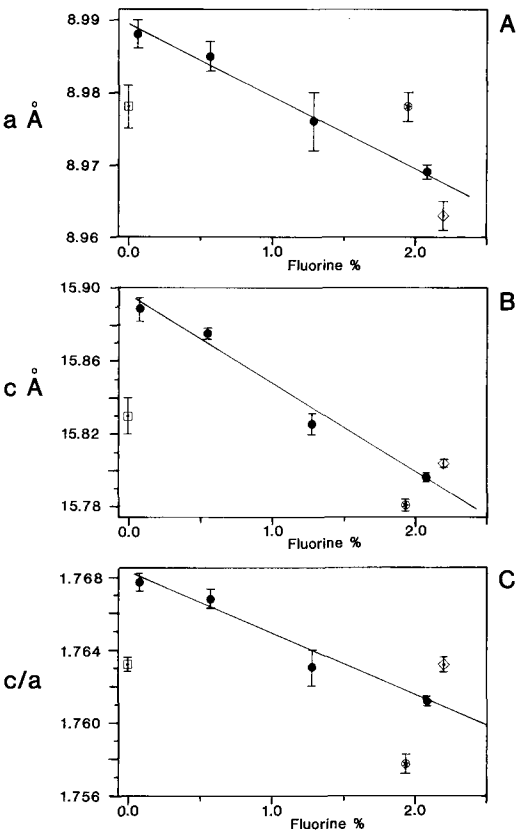

FIG. 2. Variation of cell dimensions of apophyllite in relation to fluorine content. Filled circles; fluor–hydroxy-apophyllite series. Circle with star, ammonian apophyllite GM13. Square; hyroxyapophyllite, Dunn *et al.* (1978). Diamond; fluorapophyllite, Colville *et al.* (1971).

The parameters *a*, *c* and *c*/*a* decrease linearly with increasing substitution of OH^- by F^- (Fig. 2*a*–*c*), at least up to 2% F. The contraction in *c* is 4.9 times that in *a* and for 2% F, *a* decreases by 0.2%, *c* by 0.6%, and *c*/*a* by 0.4%. For hydroxyapophyllite, extrapolation of the least-

squares regression lines gives $a = 8.989(1)$, $c = 15.894(7)$ Å, and $c/a = 1.7681(6)$. These values differ from those obtained by Dunn *et al.* (Table 1), and it is not clear if the differences are significant. An accurate determination of cell parameters thus provides a means of determining the extent to which F^- replaces OH^- in fluorapophyllite.

Diffraction data were obtained for two ammonian samples (GM13 and GM25). In this case replacement of 37% of the K^+ by NH_4^+ produced a small but significant contraction in *c* and a corresponding expansion in *a* (Fig. 2*a* and *b*). There is however a marked difference in *c/a* [$= 1.7577(5)$] compared with "normal" samples, and ammonian apophyllite may be better characterized by this ratio.

Thermal analysis

Techniques. Simultaneous thermogravimetric analysis (TGA) and differential thermal analysis (DTA) was carried out on 200 mg samples (<200 mesh, 75 μm) using a Stanton-Redcroft HT-N thermobalance fitted with a platinum-wound furnace and a STA662 DTA attachment with an inconel block. A heating rate of 10°C/min. was used throughout.

The runs were repeated, stopping the experiment after each successive reaction had peaked on the DTA curve, and the resulting powder was identified by X-ray identification. A parallel series of TGA runs was made on 10 mg samples using a Stanton-Redcroft TG770 thermobalance, and with a sample grain-size varying from fine (75 μm) powders to a single 10 mg crystal. This was to ascertain the effect of initial grain size on the crystallinity of the product and on the rate of dehydration.

Low-temperature dehydration reactions. The two reactions occurring below 600°C have previously been regarded as dehydration reactions (Aumento, 1965; Chao, 1971). The majority of samples display two distinct stages of weight loss on the TGA curves (Fig. 3), which correspond to two marked endothermic peaks on the DTA traces (Fig. 4). X-ray patterns of the partially dehydrated material differ from those of the starting material only in having slightly reduced intensities (Fig. 7); this reduction in intensity continues with progressive increase in temperature until after the second endothermic DTA reaction, when the material becomes amorphous. Infra-red studies nevertheless demonstrate that short-range order is retained. Comparison of fluorine-rich and fluorine-poor samples indicates that both DTA peaks are displaced to higher temperatures with increasing fluorine content (Fig. 5A). Fluorapophyllites give DTA peaks in the range of 310–334°C and 430–450°C, whereas the corresponding peaks for hydroxyapophyllite are in the range 300–310°C and 400–422°C respectively. The ammonian samples tend to dehydrate at slightly lower temperatures, especially for the second stage reaction. However there is not a sufficiently close correlation between dehydration temperature and fluorine content to be able to use it as a measure of fluorine content. Perhaps more interesting in this regard is that the proportion of water lost during each stage is also dependent on the fluorine content, as illustrated in Fig. 3. Isothermal runs were used to determine precisely the amount lost. Hydroxyapophyllites lose almost exactly half of their eight water molecules (7.8% by weight) during the first-stage reaction, with their remaining water molecules plus that present as OH^- during the second stage. Surprisingly, fluorapophyllites lose five of their eight water molecules (10% by weight) during the first stage, with the remaining three during the second stage. This feature constitutes a usable diagnostic, as can be seen by comparing TGA curve A (GM2, 1.99% F) with TGA curve E (GM21, 0.05% F) in Fig. 3. Ammonian apophyllites pose a complication to this simple relationship in that they inherently have higher total volatile contents than the normal K-rich apophyllites. An IR spectrum of partially dehydrated GM13 showed that the NH_4^+ absorption band at 1460 cm^{-1} had disappeared, implying that ammonia is removed during the first-stage dehydration. Nonetheless the relationship still holds as TGA curve F, an ammonian fluorapophyllite (GM13, 1.94%F), shows greater weight loss during the first-stage reaction than an ammonian hydroxyapophyllite (GM25, TGA curve G).

Ammonian apophyllites appear however to exhibit a different behaviour in their DTA curves. In general, both fluor- and hydroxyapophyllites have a second-stage endothermic reaction which is much more intense than the first lower temperature one (Fig. 4). With the ammonian varieties, the first endotherm is considerably larger and the second one reduced. In the most extreme example (Fig. 4, trace F; GM13) the second endotherm is almost negligible. GM15 is an exception in having a high weight loss (17%) and an enhanced first stage endotherm, but it is not an ammonian apophyllite (Fig. 4, curve G).

A final observation is that several samples have subsidiary peaks on the low-temperature side of the main DTA peaks. Extreme examples are GM25 and AP5 (Fig. 4J and I), where the endothermic peaks have become doublets. These are

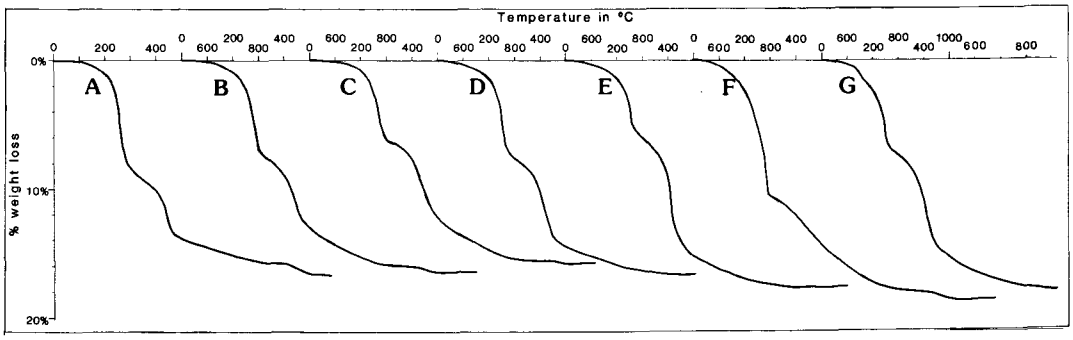

FIG. 3. Thermogravimetric analysis curves of selected apophyllites. TGA curves A–E illustrate the effects of increasing substitution of fluorine by hydroxyl. TGA curve F is the most ammonium-rich fluorapophyllite and curve G the most ammonium-rich hydroxyapophyllite. Note that TGA curve G shows an inflection during the first-stage dehydration which corresponds to an additional peak on the DTA curve (Fig. 4J). Lower temperature scales refer to TGA curves A, C, E and G. Upper temperature scales refer to TGA curves B, D and F. A—GM02, B—GM27, C—GM06, D—GM24, E—GM21, F—GM13, G—GM25.

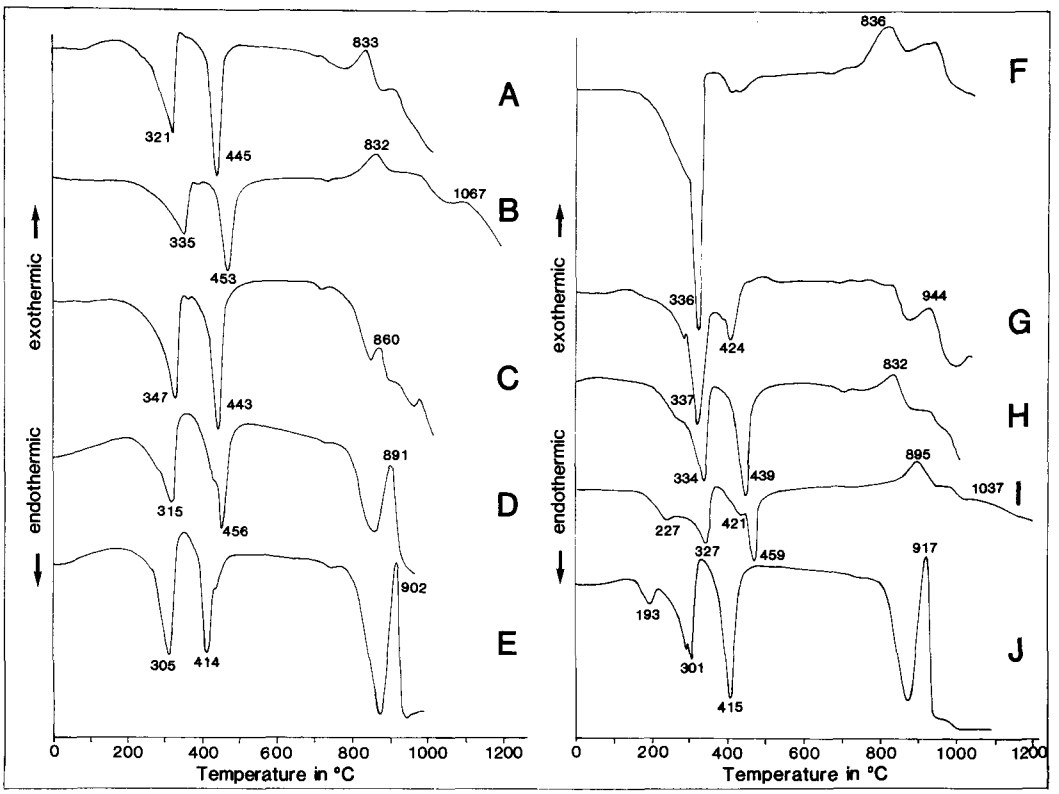

FIG. 4. Differential thermal analysis curves of selected apophyllites. DTA curves A–E illustrate the effects of progressive substitution of fluorine by hydroxyl. Curves A and B are fluorapophyllites, D and E hydroxyapophyllites. Curves F and G are ammonian apophyllites. Curves H, I and J are possible mixed-layer varieties (see text), and show the development of peak doublets. A—GM01, B—AP8, C—GM27, D—GM06, E—GM24, F—GM13, G—GM15, H—GM03, I—AP5, J—GM25.

matched by corresponding inflections in the TGA curves (Fig. 3G). Similar observations have been made by Chukrov *et al.* (1971), Vorma (1981) and Bartl and Pfeiffer (1976). X-ray powder diffraction patterns confirm that this is not a result of impurities; in any case crushed single perfectly shaped crystals yield similar DTA curves. Distortion of the lattice during grinding of powders may account for small subsidiary peaks, such as those in curves D, E and G in Fig. 4 (Peng, 1955; Morgan, pers. comm.), but not for the doublets. It is notable that of the two extreme examples, sample AP5 is intermediate in composition between fluor- and hydroxyapophyllite (with 1.43% F), and sample GM25 is an ammonian hydroxyapophyllite. One explanation is that such crystals are not homogeneous but are mixtures of fluorine-rich/fluorine-poor domains or layers (or NH_4^+-rich/NH_4^+-poor in the second case) which are reacting independently on thermal treatment. Such mixed-layer structures are not uncommon amongst layer-lattice silicates, but have not previously been proposed for apophyllite. Rouse *et al.* (1978) noted that individual apophyllites can be very inhomogeneous with respect to fluorine content, which our work also confirms; it is apparent from our microprobe studies that the same is true for potassium concentration. However, mixed-domain structures might be expected to show peak temperatures part-way between those of the end-members (Morgan, pers. comm.).

High-temperature recrystallisation reactions. Apophyllite undergoes further solid-state reactions above 600°C, but the behaviour of fluor- and hydroxyapophyllites is again different. The TGA curves demonstrate that hydroxyapophyllites undergo no further weight loss at high temperatures, all the structural OH^- having been lost during the second-stage reaction. The DTA curves show one strong exothermic reaction occurring in the temperature range 850–920°C, superimposed upon a very pronounced baseline drift (Fig. 4). The exothermic peak results from the formation of a new crystal phase, identified as high-temperature α-wollastonite by X-ray powder diffraction (Fig. 7). No other phase is present. The baseline drift is caused by sintering in the sample. Electron micrographs show the development of randomly oriented needles of high-temperature wollastonite growing like whiskers from the decomposed cleavage flakes of the parent apophyllite (Fig. 6). The size and the temperature of this exothermic peak correlates inversely with fluorine content. For instance, pure hydroxyapophyllite (AP4) and ammonian hydroxyapophyllite (GM25, curve J, Fig. 4) peak at 915°C whereas an intermediate apophyllite (GM6) with 0.95% F (curve D, Fig. 4) peaks at 891°C, and the peak is much smaller.

Fluorapophyllites behave in a more complex manner. The TGA curves of samples with more than about 0.5% fluorine exhibit a further weight loss of 0.4 to 0.8% between 920 and 940°C. This can be correlated with fluorine loss. Note however that this is only partial fluorine loss: pure fluorapophyllites contain up to 2.09% F. Prince (1971) detected HF in the evolved gases during the second dehydration stage, so some fluorine may be liberated at much lower temperatures. To clarify the position regarding fluorine loss, sample AP1 with 1.99% F was analysed for fluorine after being subject to thermal treatment at very different heating rates, (*a*) very rapidly, by plunging into a furnace at 830°C, (*b*) at the standard 10°C/min, and (*c*) very slowly bringing the temperature to 830°C. In the first case only 0.89% F was retained; in the second 1.89% F was retained at 830°C, but all the fluorine disappeared by 930°C; in the third case all the fluorine was retained. This suggests that rapid heating rates and water loss promote severe disruption of the structure, facilitating escape of fluorine during dehydration.

The DTA curves of fluorapophyllites exhibit three high-temperature peaks, compared with only one for hydroxyapophyllite. The first, at 710 to 730°C, is rather small, and marks the formation of the metastable phase $CaF_2.SiO_2$ (Marriner *et al.*, 1979). Only a small amount is produced (limited by the *ca.* 2.09% maximum available fluorine) and is poorly crystalline.

The second peak occurs at 820–840°C and marks the growth of a second new phase, identified by X-ray diffraction as low-temperature β-wollastonite. Unlike the hydroxyapophyllites, the powder at this stage remains unsintered, and electron micrographs show no growth of crystals comparable with those of the high-temperature form developed from hydroxyapophyllite. It can be seen that β-wollastonite forms at lower temperatures in the more fluorine rich apophyllites (Fig. 5B).

Above 900°C significant baseline drift on the DTA curves marks the onset of sintering, and superimposed upon this is the final DTA peak at 900–940°C, coinciding with the loss of fluorine on the TGA curves. Only high-temperature α-wollastonite was identified in the remaining powders, both the low-temperature form and $CaF_2.SiO_2$ having disappeared. In this case the high-temperature wollastonite phase forms at higher temperatures in the more fluorine-rich apophyllites (Fig. 5B).

A final technical point worth making is that it could be difficult, if DTA apparatus is not care-

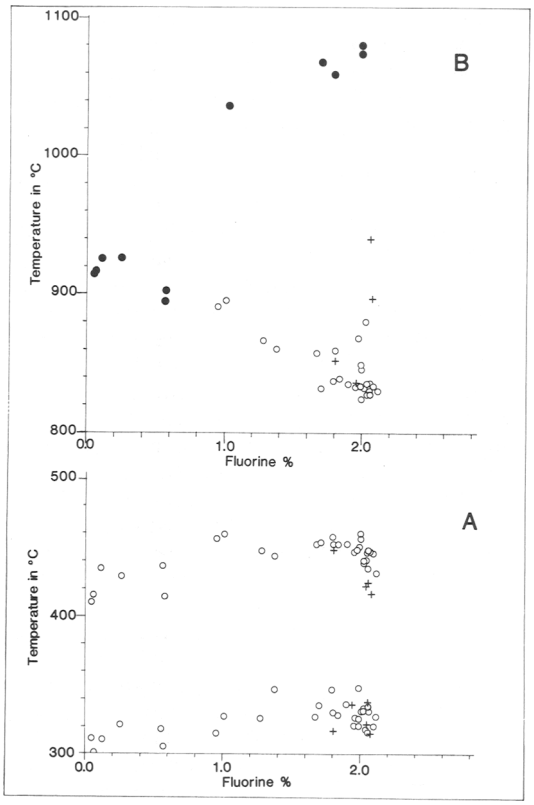

FIG. 5. Summary of thermal characteristics of apophyllites in relation to fluorine content. All determined at standard heating rate of 10°C/min. A. Low-temperature dehydration stages: DTA endothermic peaks. Open circles, fluorapophyllite—hydroxyapophyllite series. Crosses, ammonian apophyllite series. B. Temperatures of formation of low-temperature wollastonite and high-temperature wollastonite deduced from DTA exothermic peaks. Open circles, formation of low-temperature wollastonite in fluorapophyllite—hydroxyapophyllite series. Crosses, in ammonian apophyllites. Filled circles, formation of high-temperature wollastonite.

fully set-up and aligned, to distinguish the final DTA peak marking the recrystallization of high-temperature α-wollastonite from the base-line drift associated with sintering of the sample. For hydroxyapophyllite this peak is so intense it is always distinguishable; for fluorapophyllite the position is more critical—in only two of the four sets of DTA apparatus used in this study was it clearly distinguishable.

Discussion

A fascinating feature of the fluorapophyllite–hydroxyapophyllite group is the way the proportion of fluorine in the structure influences the mechanisms, temperatures and products of thermal reaction, not only during low-temperature dehydration, but also in high-temperature reactions up to almost 1000°C, and despite passing through an intermediate amorphous stage. Yet in crystallographic terms the structures of the two end-members are identical. Samples with an intermediate fluorine content in general show a behaviour between the two extremes.

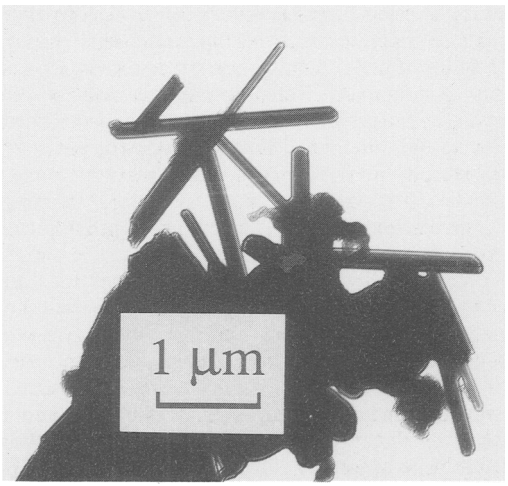

FIG. 6. Electron photomicrograph illustrating randomly oriented needles of high-temperature wollastonite formed from hydroxyapophyllite.

Fluorine clearly imparts considerable stability to the structure. Reactions in fluorapophyllites are all displaced to higher temperatures relative to those in hydroxyapophyllites. During the first-stage dehydration, fluorapophyllites are able to lose one extra water molecule compared with hydroxyapophyllites, without precipitating breakdown of the structure. In detail the difference in behaviour is observed at *ca.* 0.95% fluorine (i.e. 45% site occupancy). Thus hydroxyapophyllites having less than this amount need to retain half their water molecules to maintain the structure after the first dehydration stage, but become amorphous during the second dehydration stage and remain so until sintering occurs at ca. 900°C with the formation of new crystallites of high-temperature α-wollastonite.

Apophyllites with more than 0.95% F not only breakdown at progressively higher temperatures with increasing fluorine content, but the higher temperature reactions are also different. After

passing through an amorphous stage, the metastable phase $CaF_2.SiO_2$ forms and is rapidly joined at slightly higher temperatures by the low temperature β-form of wollastonite. No sintering occurs and no growth of new crystallites is visible under the electron microscope. The inference must be that, during the second dehydration stage, selected parts of the fluorapophyllite structure are being preserved which are closely related to that of low-temperature wollastonite and that can be readily rebuilt into the wollastonite structure. Significantly, during attempts to obtain single crystal data on the metastable $CaF_2.SiO_2$ phase by electron diffraction, patterns consistent with low-temperature wollastonite were repeatedly obtained, even on material which showed no evidence of low-temperature wollastonite using X-ray diffractometry. Attempts to increase the crystallinity of the phase by using coarser starting material or longer heating periods were unsuccessful. The implication is that very little long-range movement of ions had taken place and that no new crystallites were being formed: the wollastonite phase may be a poorly formed relic of parts of the original apophyllite structure. On the other hand, the wollastonite phase appears at lower temperatures in the more fluorine-rich samples, and the corresponding DTA peaks are sharper, suggesting that fluorine mobility is indirectly aiding the growth of wollastonite domains. At the same time increased fluorine content enables the wollastonite phase to be preserved to higher temperatures. If fluorine is lost (as HF) during rapid second-stage dehydration, neither the β-wollastonite nor the $CaF_2.SiO_2$ phase are preserved. Breakdown of $CaF_2.SiO_2$ is accompanied by simultaneous disappearance of low-temperature wollastonite. The high temperature α-variety of wollastonite recrystallizes from the disrupted areas of the low-temperature form, but at higher temperatures and as crystallites.

The dehydration behaviour of apophyllites observed in this study bears upon the problem of whether there are one or two structural sites for water molecules in the crystal lattice. Structural determinations indicate unequivocally that there is only one (Colville *et al.*, 1971; Prince, 1971; Bartl and Pfeifer, 1976) whereas the two-stage dehydration behaviour suggests two such sites (Chao, 1971). However, taking the apophyllite group as a whole, the proportion of water lost during the first and second dehydration stages, respectively, is highly variable, and it would be unrealistic to apportion water molecules to more than one site. Instead, the proportion lost at each stage is more directly linked to the fluorine content. The key to the problem was provided by Lacy (1965): the high activation energy of the second stage reaction indicates that Si–O bonds are being ruptured, with breakdown of the lattice, liberating the remaining water, the OH ions and some of the fluorine. Only one site is necessary for the water molecules, as the second stage reaction is not strictly a dehydration but is primarily a destruction of the apophyllite structure with accompanying liberation of the remaining water and hydroxyl.

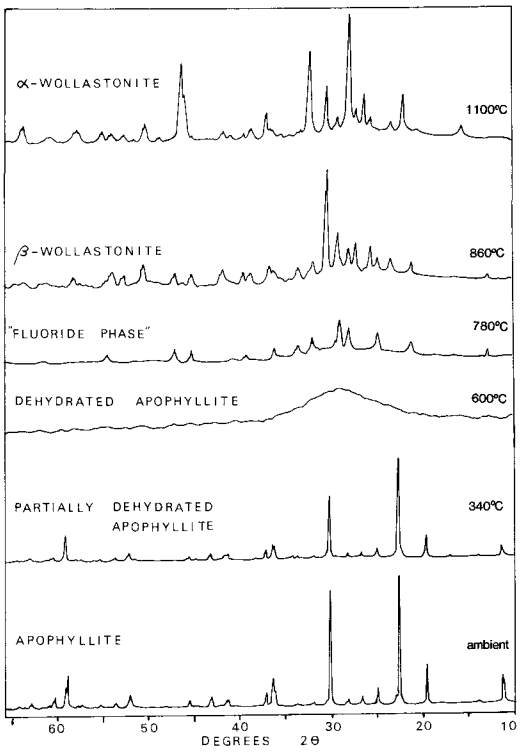

FIG. 7. X-ray diffractograms of fluorapophyllite (AP01) and its dehydration products.

Finally, the discovery of ammonian varieties of apophyllite during this investigation extends the range of silicates where significant replacement of potassium by the ammonium ion occurs. Such ammonian apophyllites can be distinguished from normal apophyllites by their DTA and IR curves. In normal fluor- and hydroxyapophyllites the second endothermic peak is normally larger than the first. In ammonian varieties the first DTA peak is larger and the ratio of the first to the second peak increases with increasing substitution of NH_4^+ for K^+ because the NH_4^+ is liberated during the first stage of dehydration, and hence the higher the NH_4^+ concentration the greater the disruption of the lattice.

Acknowledgements

We thank the British Museum (Natural History), University of Birmingham, Bedford and University Colleges, London, and Prof. R. A. Howie for supplying samples used in this study. We are grateful for the generous use of instrumental facilities at the British Geological Survey, London, the Chemistry Department, Aberdeen, the EM Unit, RHBNC and the Crystallography Department, Birkbeck College, and to Dr N. Walsh, Dr A. Hall, Dr F. Glasser, R. N. Wilson, R. Williams and R. Fuge for analytical assistance. Prof. H. F. W. Taylor, Prof. R. A. Howie, Mr. E. D. Lacy and Dr D. Morgan are thanked for advice and constructive comments.

References

Aumento, F. (1965) *Thermal transformations of selected zeolites and related hydrated silicates*. PhD Thesis, Dalhousie University, Halifax, Canada.

Bartl, H. and Pfeifer, G. (1976) Neutronen beigungsanalyse des Apophyllite $KCa_4(Si_4O_{10})_2(F/OH).8H_2O$. *Neues Jahrb. Mineral. Mh.*, 58–65.

Chao, G. Y. (1971) Refinement of the crystal structure of apophyllite. II. Determination of the hydrogen positions by X-ray diffraction. *Am. Mineral.* **58**, 1234–42.

Chukrov, P. V., Yermilova, L. P. and Rudnitskaya, Y. S. (1971) Nature of water in apophyllite. *Nouv. Denn. Mineral. SSSR., Akad. Nauk SSSR Mineral. Muz.* **20**, 221–5.

Colville, A. H., Anderson, C. P. and Black, P. M. (1971) Refinement of the crystal structure of apophyllite. I. X-ray diffraction and physical properties. *Am. Mineral.* **53**, 1222–33.

Duit, W., Jansen, J. B. H., Van Breemen, A. and Bos, A. (1986) Ammonium micas in metamorphic rocks as exemplified by Dome de L'Agout (France). *Am. J. Sci.* **286**, 702–32.

Dunn, P. J., Rouse, R. C. and Norberg, J. A. (1978) Hydroxyapophyllite, a new mineral and a redefinition of the apophyllite group, I. Description and nomenclature. *Am. Mineral.* **63**, 196–9.

Lacy, E. D. (1965) Factors in the study of metamorphic reaction rates. In *Controls of Metamorphism* (Pitcher, W. S. and Flinn, G. W., eds.) 140–54. Oliver and Boyd, London.

Langford, J. I. (1971) Powder pattern programs. *J. Appl. Crystallogr.* **4**, 259–60.

Mann, L. T. (1963) Spectrophotometric determination of nitrogen in total micro-kjeldahl digest. *Anal. Chem.* **35**, 2179–82.

Marriner, G. F., Langford, J. I. and Tarney, J. (1979) Crystal data for calcium fluoride silicon oxide ($CaF_2.SiO_2$), a dehydration product of fluorapophyllite. *J. Appl. Crystallogr.* **12**, 131–2.

Matsueda, H., Miura, Y. & Rucklidge, J. (1981) Natroapophyllite, a new orthorhombic sodium analog of apophyllite. I. Description, occurrence and nomenclature. *Am. Mineral.* **66**, 410–15.

Miura, Y., Kato, T., Rucklidge, J. and Matsueda, H. (1981) Natroapophyllite, a new orthorhombic sodium analog of apophyllite. II. Crystal structure. Ibid. **66**, 416–23.

Peng, C. J. (1955) Thermal analysis study of the natrolite group. Ibid. **40**, 834–56.

Prince, E. (1971) Refinement of the crystal structure of apophyllite. III. Determination of the hydrogen positions by neutron diffraction. Ibid. **56**, 1243–51.

Reed, S. J. B. (1976) *The electron microprobe*. Cambridge University Press.

Rouse, R. C., Peacor, D. R. and Dunn, P. J. (1978) Hydroxyapophyllite, a new mineral and a redefinition of the apophyllite group. II. Crystal structure. *Am. Mineral.* **63**, 199–202.

Sarig, S. (1973) Simultaneous TG, DTG and DTA analysis in controlled inert gas flow for the determination of desquification steps of polyhydrated sulphates. *Thermochim. Acta* 297–301.

Solomon, G. C. and Grossman, G. R. (1988) NH_4^+ in pegmatitic feldspars from the Southern Black Hills, South Dakota. *Am. Mineral.* **73**, 818–21.

Taylor, H. F. W. and Náray-Szabò, St. (1931) The structure of apophyllite. *Zeits. Kristallogr.* **77**, 148–56.

Vorma, A. (1961) A new apophyllite occurrence in Viipuri Rapkivi area. *Bull. Comm. Geol. Finlande*, **196**, 399–404.

Walsh, N. (1979). The simultaneous determination of major, minor and trace constituents of silicate rocks using inductively coupled plasma. *Spectrochim. Acta*, **35**, 107–11.

——, Howie, R. A. (1980) The evaluation of the performance of ICP for the determination of major and trace constituents of silicate rocks. *Mineral. Mag.* **43**, 967–74.

Yamamoto, T. and Nakahira, M. (1966) Ammonium ions in sericites. *Am. Mineral.* **51**, 1775–8.

[*Manuscript received 13 October 1989; revised 29 May 1990*]